

DTIC  
SELECTED  
JAN 03 1994  
S F D

AN INVESTIGATION OF THE AFIT  
2-INCH SHOCK TUBE AS A FLOW  
SOURCE FOR SUPERSONIC TESTING

THESIS  
Kevin M. Vlcek  
Captain, USAF

AFIT/GA/ENY/94D-1

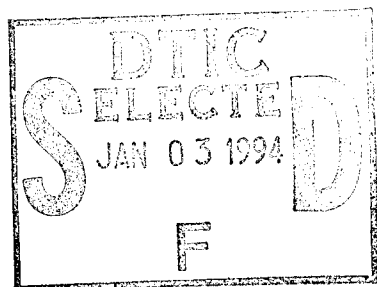
This document has been approved  
for public release and sale; its  
distribution is unlimited.

DEPARTMENT OF THE AIR FORCE  
AIR UNIVERSITY  
**AIR FORCE INSTITUTE OF TECHNOLOGY**

Wright-Patterson Air Force Base, Ohio

19941228 071

AFIT/GA/ENY/94D-1



Accession For	
NTIS CRA&I	<input checked="" type="checkbox"/>
DTIC TAB	<input type="checkbox"/>
Unannounced	<input type="checkbox"/>
Justification	
By _____	
Distribution/	
Availability Codes	
Dist	Avail and/or Special
A-1	

AN INVESTIGATION OF THE AFIT  
2-INCH SHOCK TUBE AS A FLOW  
SOURCE FOR SUPERSONIC TESTING

THESIS  
Kevin M. Vlcek  
Captain, USAF

AFIT/GA/ENY/94D-1

UNCLASSIFIED//FOR OFFICIAL USE ONLY

The views expressed in this thesis are those of the author and do not reflect the official policy or position of the Department of Defense or the U. S. Government.

AFIT/GA/ENY/94D-1

AN INVESTIGATION OF THE AFIT 2-INCH SHOCK TUBE AS A FLOW  
SOURCE FOR SUPERSONIC TESTING

THESIS

Presented to the Faculty of the Graduate School of Engineering  
of the Air Force Institute of Technology  
Air University  
In Partial Fulfillment of the  
Requirements for the Degree of  
Master of Science in Astronautical Engineering

Kevin M. Vlcek, B.S.  
Captain, USAF

December, 1994

Approved for public release; distribution unlimited

## *Preface*

The purpose of this thesis was to determine the usefulness of the AFIT 2-inch shock tube for establishing supersonic flow. Tests were run both with an endwall attached to the end of the shock tube and with a Mach 3 nozzle attached. The Mach numbers of the incident shock waves and pressures behind the incident and reflected shock waves were compared to theoretical values obtained from the ideal shock tube relations. With the nozzle attached, periods of steady flow were established at the nozzle exit. The duration of steady flow for each run was measured to determine the range of test times available.

I would like to express my appreciation to the people whose guidance and advice were invaluable to the successful completion of this study. In particular, my advisor Lt Col Jerry Bowman who provided me with timely direction when needed to complete this work. My thanks to Maj John Doty and Dr Philip Beran for their advice and support as thesis committee members. Additionally, I thank Jack Tiffany and the staff at the AFIT Model Fabrication shop for their efforts in constructing the nozzle.

Kevin M. Vlcek

## *Table of Contents*

	Page
Preface . . . . .	ii
List of Figures . . . . .	v
List of Tables . . . . .	vi
List of Symbols . . . . .	vii
Abstract . . . . .	viii
I. Introduction . . . . .	1
Problem Statement . . . . .	2
Background . . . . .	2
II. Theory . . . . .	5
Shock Tube Operation . . . . .	5
Ideal Shock Tube Relations . . . . .	8
III. Experimental Apparatus and Procedure . . . . .	11
Shock Tube . . . . .	11
Pressure Transducers . . . . .	12
Datalab DL1200 . . . . .	13
Bottle Farm . . . . .	14
Procedure . . . . .	14

	Page
IV. Results . . . . .	15
Data Collection . . . . .	15
Comparison with Theory . . . . .	18
Test Times . . . . .	26
Nozzle Mach Numbers . . . . .	33
V. Conclusions and Recommendations . . . . .	34
Conclusions . . . . .	34
Recommendations . . . . .	35
Appendix A. Data . . . . .	36
Bibliography . . . . .	38
Vita . . . . .	39

## *List of Figures*

Figure	Page
1. x-t Diagram and Pressure and Temperature Plots for the Shock Tube Prior to Shock Wave Reflection . . . . .	6
2. x-t Diagram and Pressure and Temperature Plots for the Shock Tube After Shock Wave Reflection . . . . .	7
3. Pressure Transducer Locations . . . . .	16
4. Pressure History at the Nozzle Entrance (Pressure Transducer 5) . . . . .	17
5. Pressure History at the Nozzle Exit (Pressure Transducer E) . . . . .	17
6. Pressure History at the Nozzle Exit for an Unstarted Nozzle . . . . .	18
7. Incident Shock Wave Mach Number Versus Diaphragm Pressure Ratio Compared to Ideal Shock Tube Relations . . . . .	20
8. Incident Shock Strength Versus Diaphragm Pressure Ratio Compared to the Ideal Shock Tube Relations . . . . .	21
9. Incident Shock Strength Versus Mach Number . . . . .	21
10. Reflected Shock Strength Versus Diaphragm Pressure Ratio Compared to the Ideal Shock Tube Relations . . . . .	22
11. Incident Shock Mach Number Versus Reflected Shock Strength Compared to the Ideal Shock Tube Relations . . . . .	23
12. Baer's Figure 11, $P_4/P_1$ vs Mach Number . . . . .	24
13. Baer's Figure 12, $P_5/P_1$ vs Mach Number . . . . .	25
14. Uda's Figure 22, Diaphragm Pressure Ratio Experimental Data Points Compared to Ideal Gas Theory Curve for the He/Air System . . . . .	27
15. Uda's Figure 23, Reflected Shock Pressure Ratio Experimental Data Points Compared to Equilibrium and Ideal Air Theory Curves . . . . .	28
16. Measured Test Times as a Function of the Pressure Ratio Across the Nozzle	29
17. Pressure History at the Location of Pressure Transducer B Upstream of the Nozzle . . . . .	32



*List of Tables*

Table		Page
1.	Data for the Case of the Nozzle Attached . . . . .	37
2.	Data for the Case of the Plate/Endwall Attached . . . . .	37

## *List of Symbols*

### Symbol

- $a$  speed of sound
- $A_t$  area of the nozzle throat
- $\dot{m}$  mass flow rate
- $M$  Mach number
- $P$  pressure
- $R$  gas constant
- $T$  temperature
- $\gamma$  ratio of specific heats

### Subscript

- 1 initial low pressure driven gas conditions
- 2 region between the shock wave and the contact surface
- 3 region of expanded driver gas behind the contact surface
- 4 initial driver gas conditions
- 5 region behind the reflected shock wave
- e conditions in the nozzle exit plane

*Abstract*

An investigation of the AFIT high pressure shock tube was conducted to determine how closely it followed ideal shock tube theory and to determine the available test times for an attached Mach 3 nozzle. The driver section was five feet (1.52 m) long and the driven section was 25 feet (7.62 m) long. The driver gas used for this study was helium while the driven gas was atmospheric air.

The pressure rise measured behind the incident shock wave was, on average, 30% lower than predicted by the ideal shock tube relations. Behind the reflected shock, the pressure rise was 65% lower than predictions based on initial driver gas pressure. Due to supply pressure limits and lower than predicted pressures behind the shock waves, fully expanded flow in the Mach 3 nozzle was not attained. However, steady overexpanded flows of Mach 2.74–2.96 were observed for periods of 4–12 milliseconds.

# AN INVESTIGATION OF THE AFIT 2-INCH SHOCK TUBE AS A FLOW SOURCE FOR SUPERSONIC TESTING

## *I. Introduction*

Since its introduction in 1949, the shock tube has become an increasingly popular tool for a large variety of experiments from supersonic aerodynamics to heat transfer to supersonic combustion. Almost any endeavor that requires a high temperature gas or supersonic flow could be designed to be tested in a shock tube. A significant limiting factor for shock tube use is the short test times available, on the order of milliseconds. These short test times require sophisticated data collection techniques and a need to rely to some extent on analytical predictions of the behaviour of the flow. A shock tube is a relatively inexpensive but effective way to perform many studies if the short test times are satisfactory to complete data collection. Also, use of a shock tube avoids material problems associated with longer duration, high temperature tests. Since its acquisition, the AFIT 2-inch shock tube, also known as the AFIT high speed or high pressure shock tube, has been used for many studies in which it was necessary to produce supersonic flow or to create a stagnant test region at elevated temperatures.

### *Problem Statement*

The purpose of this investigation was twofold. The first step was to characterize the AFIT 2-inch shock tube as compared to ideal shock tube relations. Next, the range of obtainable test times was determined for the shock tube with a Mach 3 nozzle attached to the end of the driven section.

### *Background*

Since AFIT has acquired the 2-inch shock tube, many research projects have been conducted using it as a tool to produce the flow or temperatures required. The researchers have relied to various degrees on the assumption that the ideal shock relations applied to their studies. Few compared their measured variables to those predicted by the ideal relations to verify their assumption of ideal shock waves.

Uda (1968) conducted a study on boron ignition with the Aero Propulsion Lab's 3-inch shock tube. His figures depict only 15-20% weaker incident shock strength and virtually no pressure loss in the region behind the reflected shock. Adjusted for the measured shock strength, his pressure data follows the ideal relations. This lends credence to his reliance on the ideal shock relations to determine the temperatures behind the reflected shock waves. Uda's data is included for comparison in Chapter 4. Jones (1969) continued this work in the AFIT 2-inch shock tube. Jones also relied on the ideal relations to determine the temperature behind the reflected shock although he made no comparison of theory to actual data. Without a comparison of his pressure data to theory, there was no basis to assume the pressure rises

he measured followed the ideal relations and extending this to assumption of ideal flow to determine the temperatures.

Farnell (1980) used the 2-inch shock tube to study iodine dissociation. Although “35 test runs were made to establish operational integrity,” no data or test results were given other than “excellent test repeatability.” No justification was made for using ideal relations for calculating the temperature behind the reflected shock wave. Baer (1982) conducted similar research on iodine emission in the 2-inch shock tube. His test data indicates a significant loss of incident shock strength and speed compared to predictions by the ideal shock relations. His figure (see Fig 13) of the reflected shock strength versus Mach numbers centered around the prediction curve which indicates that the reflected shock wave, on average, attained its predicted pressure rise. The fact that a third of the data points showed pressure ratios greater than the theoretical limit was not addressed but would seem to indicate an error in measured shock wave speed or strength. Baer’s data is also included in Chapter 4.

In each of these studies, the ideal shock relations were used to obtain the temperature behind the reflected shock for lack of a more accurate method. The present study measured pressures behind the incident and reflected shock waves to determine how closely the AFIT 2-inch shock tube follows the ideal shock relations. Lower than ideal pressures were expected and it was believed that the temperature would experience proportionally lower values. Tests were run both with a Mach 3 nozzle and with a flat plate attached to the end of the shock tube to serve as an endwall for shock wave reflection. The nozzle was expected to allow a portion of the shock wave to pass through the throat resulting in lower pressures behind the reflected

shock wave than predicted by the ideal relations. Test times in the nozzle exit plane were then measured to determine the range of test times available for the given shock tube and nozzle for future experiments.

## *II. Theory*

### *Shock Tube Operation*

A shock tube is a device in which a moving, normal shock wave can be produced. A mylar or metal diaphragm separates a high pressure 'driver' gas from a lower pressure 'driven' or test gas. When the diaphragm is caused to rupture, compression waves spontaneously move down the tube, quickly coalescing into a shock front. As the shock wave moves down the driven section of the shock tube, it compresses the gas it passes through, increasing the driven gas's temperature and pressure and accelerating the gas to a velocity nearly as fast as the shock wave's velocity. At the same time, an expansion fan moves into the driver section with the effect of lowering the driver gas temperature and pressure. A 'contact surface,' separating driver and driven gases at equal pressure, travels into the driven section at the same velocity as the gas behind the incident shock wave. Figure 1 is an x-t diagram of the flow through the shock tube with relative pressure and temperature plots of the different regions for a time prior to the shock's reflection. Figure 2 shows the conditions for a time after the shock wave has reflected.

The shock wave travels the length of the tube and reflects from the endwall or the mouth of the nozzle, if attached, and starts back up the tube. The gas behind the reflected shock, having been compressed twice, forms a pocket of high pressure, high temperature gas that may be expanded through a nozzle to accelerate the gas to higher Mach numbers than those achievable behind the incident shock wave. Test time ends when the flow in the test section,



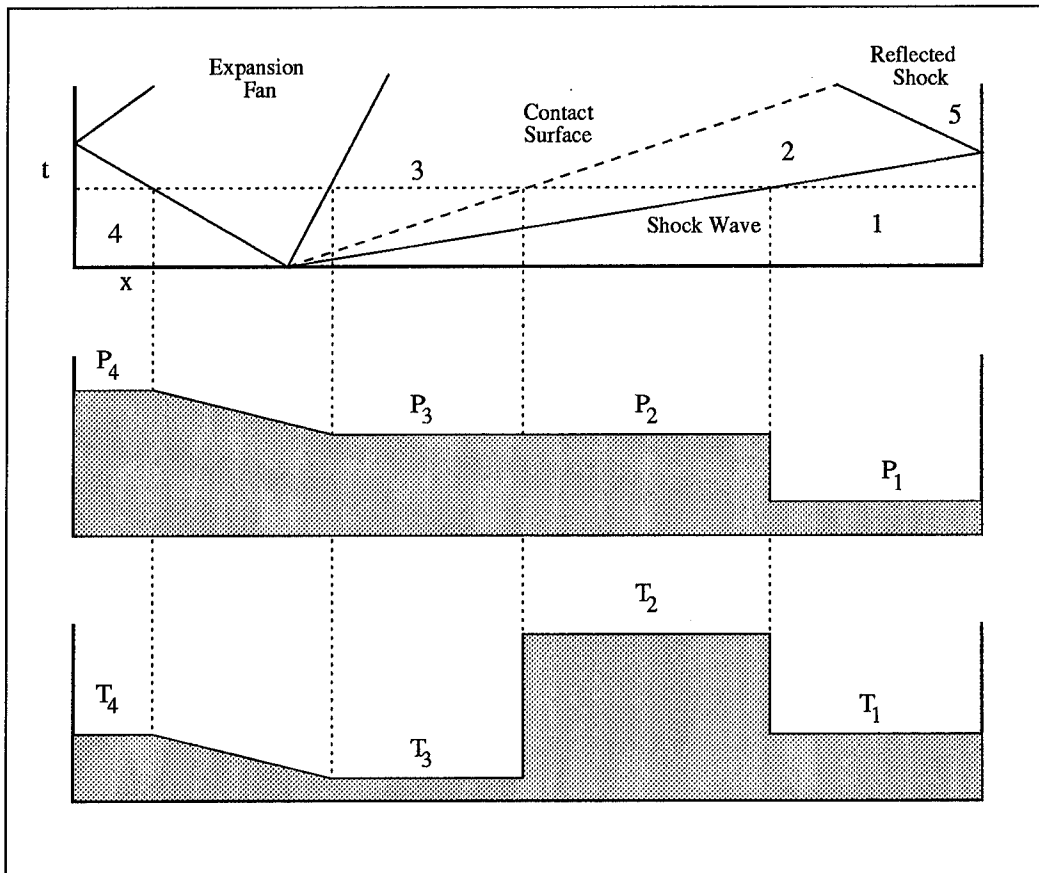


Figure 1.  $x$ - $t$  Diagram and Pressure and Temperature Plots for the Shock Tube Prior to Shock Wave Reflection

at the nozzle exit, destabilizes. That is, the pressure makes an abrupt change from its relatively constant test time value. If the contact surface flows through the nozzle before the flow destabilizes and the driver gas differs from the driven gas, the test time ends with the contact surface arrival. If the same gas is used for driver and driven gases, data collection should still be terminated at contact surface arrival if the lower temperature gas would influence the desired data. For more details, the reader is referred to Gaydon and Hurle (1963), Hall (1958) or similar references discussing shock tube operation.

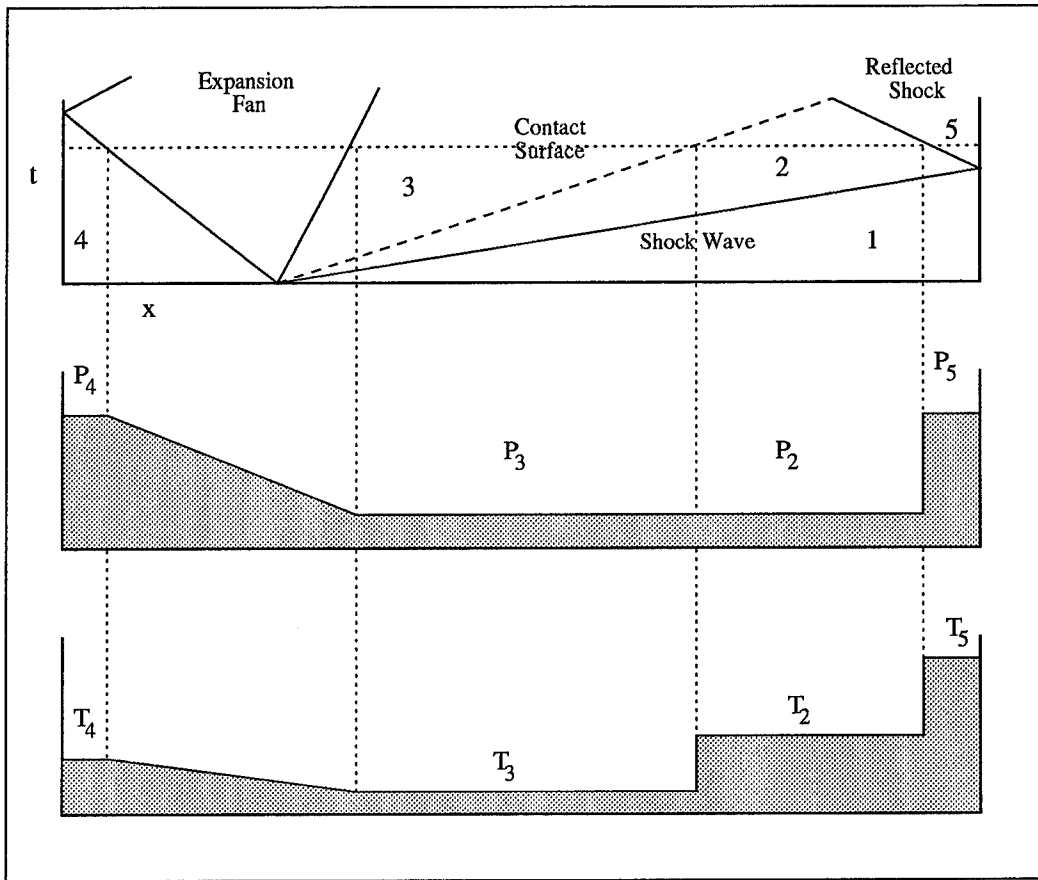


Figure 2.  $x$ - $t$  Diagram and Pressure and Temperature Plots for the Shock Tube After Shock Wave Reflection

During its operation, different regions are created in the shock tube as the shock and expansion waves interact with the gases. These different regions contain the driver and driven gases at different temperatures and pressures, and are designated as

- Region 1 initial low pressure driven gas conditions
- Region 2 compressed driven gas between the shock wave and the contact surface
- Region 3 expanded driver gas behind the contact surface
- Region 4 initial driver gas conditions
- Region 5 conditions behind the reflected shock wave
- Region e conditions in the nozzle exit plane

### *Ideal Shock Tube Relations*

The following basic equations relating the pressures and temperatures in the different regions have been derived for the case of ideal gases (Gaydon, 1963). Assumptions made in their derivation include: constant specific heat ratios ( $\gamma$ ), no dissociation or ionization, no heat exchange in the shock wave, perfect diaphragm rupture, negligible boundary layer, and 100% endwall reflection.

The standard relations between the pressure and temperature ratios across a normal shock wave and the shock's Mach number may be found in any text treating shock waves and are

$$\frac{P_2}{P_1} = \frac{2\gamma M^2 - (\gamma - 1)}{\gamma + 1} \quad (1)$$

$$\frac{T_2}{T_1} = \frac{[2\gamma M^2 - (\gamma - 1)][(\gamma - 1)M^2 + 2]}{(\gamma + 1)^2 M^2} \quad (2)$$

where  $P_x$ ,  $T_x$  represent, respectively, the pressure and temperature in region  $x$ .  $M$  is the Mach number of the incident shock wave and  $\gamma$  is the specific heat ratio of the driven gas. The pressure ratio  $P_2/P_1$  defines the strength of the shock wave. Although not necessary for

the present study, the relations for temperatures are included for consideration in the losses incurred in the shock tube.

For a given diaphragm pressure ratio, the Mach number of the incident shock wave may be predicted from

$$\frac{P_4}{P_1} = \frac{2\gamma_1 M^2 - (\gamma_1 - 1)}{\gamma_1 + 1} \left[ 1 - \frac{\gamma_4 - 1}{\gamma_1 + 1} \frac{a_1}{a_4} \left( M - \frac{1}{M} \right) \right]^{-\left(\frac{2\gamma_4}{\gamma_4 - 1}\right)} \quad (3)$$

Conditions across the reflected shock wave are predicted from

$$\frac{P_5}{P_2} = \frac{\frac{\gamma+1}{\gamma-1} + 2 - \frac{P_1}{P_2}}{1 + \frac{\gamma+1}{\gamma-1} \frac{P_1}{P_2}} \quad (4)$$

$$\frac{T_5}{T_2} = \frac{P_5}{P_2} \left( \frac{\frac{\gamma+1}{\gamma-1} + \frac{P_3}{P_2}}{1 + \frac{\gamma+1}{\gamma-1} \frac{P_3}{P_2}} \right) \quad (5)$$

where  $\gamma$  is again that for the driven gas.

The solution for the conditions behind the reflected shock in terms of the incident shock Mach number and initial driven gas conditions are predicted from

$$\frac{P_5}{P_1} = \left[ \frac{2\gamma M^2 - (\gamma - 1)}{\gamma + 1} \right] \left[ \frac{3\gamma - 1}{(\gamma - 1)M^2 + 2} \right] \quad (6)$$

$$\frac{T_5}{T_1} = \frac{[2(\gamma - 1)M^2 + (3 - \gamma)][(3\gamma - 1)M^2 - 2(\gamma - 1)]}{(\gamma + 1)^2 M^2} \quad (7)$$

It should be stressed that these are only predictions since the true values may be affected by losses in the rupturing process, boundary layer growth, and other real gas effects and can

only be determined from accurate measurements. In most cases the measured conditions will be less than those arrived at with the preceding relations.

### *III. Experimental Apparatus and Procedure*

The instruments employed in this study included a shock tube, a Mach 3 nozzle, a flat plate to serve as an endwall, electronic collecting and processing instrumentation, and support equipment.

#### *Shock Tube*

The AFIT 2-inch shock tube is constructed of 2-inch (5.08 cm) inner diameter, type 321 stainless steel tubing. Construction in five foot (1.524 m) sections allows the lengths of driver and driven sections to be tailored to the needs of the experiment being run. For this study, the driver section was five feet and the driven section was 25 feet (7.62 m) in length. The driver gas was helium while the driven gas was atmospheric air. Both aluminum and stainless steel diaphragms in various thicknesses were used to allow for a variation in the diaphragm pressure ratio,  $P_4/P_1$ . The quality of the diaphragms was less than desirable. The breaking strengths in a given batch varied as much as 400 psi (2.8 MPa), leading to numerous premature ruptures and loss of time and helium.

This shock tube was designed to be run with two diaphragms, although it could also be operated using just one. With a single diaphragm, the driver pressure was slowly increased until the diaphragm could no longer support the pressure difference across it, causing it to rupture. When using two diaphragms, the pressure in the driver section and the region between the two diaphragms (double diaphragm or DD section) was raised to approximately 90% of

the downstream diaphragm's capability. The double diaphragm section was then sealed off and the driver section was pressurized to the desired pressure, typically 90% of the upstream diaphragm's capability.

Diaphragm rupture was caused by evacuating the DD region. This increased the pressure differential across the upstream diaphragm beyond its strength. The upstream diaphragm ruptured, succeeded by the downstream one. An alternate method used to fire the shock tube was to reopen the passage between the DD region and the driver section. In this way, the downstream diaphragm rupture preceded the upstream rupture. Both methods were used without noticeable difference in the strengths of the shocks produced.

#### *Pressure Transducers*

Four Endevco 8510B-500, 0–500 psi (0–3.45 MPa) pressure transducers were used to record the pressure changes throughout the shock tube and nozzle. Two were located at distances of 10 and 20 feet (3.048 and 6.096 meters) upstream of the nozzle, the third was located just above the nozzle entrance, and the fourth was located in the nozzle exit plane. All four Endevco transducers' signals were fed through an Endevco 4423 PR signal conditioner prior to flowing into the Datalab DL1200 for processing and recording. The Endevco pressure transducers were calibrated using a dead weight calibration technique with an Ametek model HK-500 pneumatic pressure tester.

A Viatran model 104, 0–2000 psi (0–13.79 MPa) pressure transducer was located in the shock tube driver section. Driver pressure output voltages were fed through a Power/Mate

Corp BP 76 power supply for amplification before being processed by the DL1200. This pressure transducer was calibrated using a Futurecraft Corp Cali-Kit number 90255.

### *Datalab DL1200*

The Datalab DL1200 Multichannel Waveform Recorder is a high-speed, analog-to-digital instrument used to record the voltages from the pressure transducers. Some error was noted in the output of the DL1200. The maximum deviation in the output voltage from input voltages of 0–5 volts was 102 millivolts noted on channel 8. Since AFIT lacks the equipment necessary to calibrate the DL1200, it was decided to use the five best channels and continue. Of the five channels used, the maximum absolute deviation was 41 millivolts. The maximum relative deviation was 1.9%. The voltage errors were all below input voltage. All of the electronic equipment was powered on 24 hours a day to avoid a shift in the calibration curve slope during warm-up.

The DL1200 was set to trigger off the pressure rise seen by a selected transducer. Trigger set up, sample rate, and channel setup were all adjustable. After recording a data series, it was analyzed with the use of Data Analysis and Display Software (DADiSP) worksheet. The DADiSP worksheet uses the form of a spreadsheet in displaying, manipulating, and analyzing data. A worksheet consists of a number of windows (1–100) where the data can be displayed concurrently in different stages from raw data to final calibrated results in any choice of units. More information about DADiSP and its capabilities can be found in the DADiSP manual (DADiSP, 1992).



### *Bottle Farm*

Bottled gas was used to pressurize the driver section of the shock tube. A five bottle farm was established to permit complete depletion of the helium bottles. Although the bottles of helium were delivered at 2500 psi (17.23 MPa), the pressure regulator in the driver supply system limited driver pressures to approximately 1500 psi (10.34 MPa).

### *Procedure*

Diaphragms were selected based upon the desired driver-to-driven pressure ratio,  $P_4/P_1$ , and put into place. The DL1200 was armed with desired sampling rate and trigger channel information to capture the data of interest. The driver section was then pressurized and fired as described previously. After the run, air at 100 psi (0.69 MPa) was blown through the shock tube to force out any remaining helium and assure the remaining gas in the tube was 100% air for the next run. The spent diaphragms were then removed, inspected for quality of rupture, and replaced. Quality of diaphragm ruptures varied from run to run. Those runs for which the diaphragms failed to 'petal back' were not included in the data pool for calculations or plots since the data was inherently flawed. The collected data was saved as a data file and later imported into a DADiSP worksheet shell designed to convert the raw voltage data into the desired pressure graphs representing the flow of waves and gases within the shock tube.

## *IV. Results*

Data collection was performed with the aid of DADiSP to convert voltages from the pressure transducers into pressures. The data could then be read from the pressure histories depicted by each transducer. Evaluation of the data was split into two categories: a comparison to the theory of an ideal shock tube and the determination of the test times available for the current configuration. This was followed by a check of the Mach numbers of the flow in the nozzle exit plane.

### *Data Collection*

For a given driver-to-driven pressure ratio, ideal shock relations, Equations 1, 3, and 6, were used to predict the ideal values of  $P_2$ ,  $M$ , and  $P_5$ . The actual velocity of the shock wave was determined by dividing the distance between two pressure transducers by the time it took the shock wave to traverse that distance. The velocity was then divided by the sound speed of region 1 to find the actual Mach number. Figure 3 shows the locations of the pressure transducers in the shock tube. Transducers A, B, and 5 were used to trigger data acquisition on different data runs and were used to calculate shock wave velocities. Transducers A and B measured the pressure behind the incident shock wave  $P_2$ . Transducer 5 measured the pressure behind the reflected shock wave  $P_5$ , or equivalently, the pressure at the nozzle entrance. Transducer E measured the pressure in the nozzle exit plane. The pressures from transducers 5 and E were used to determine the Mach number of the nozzle flow.

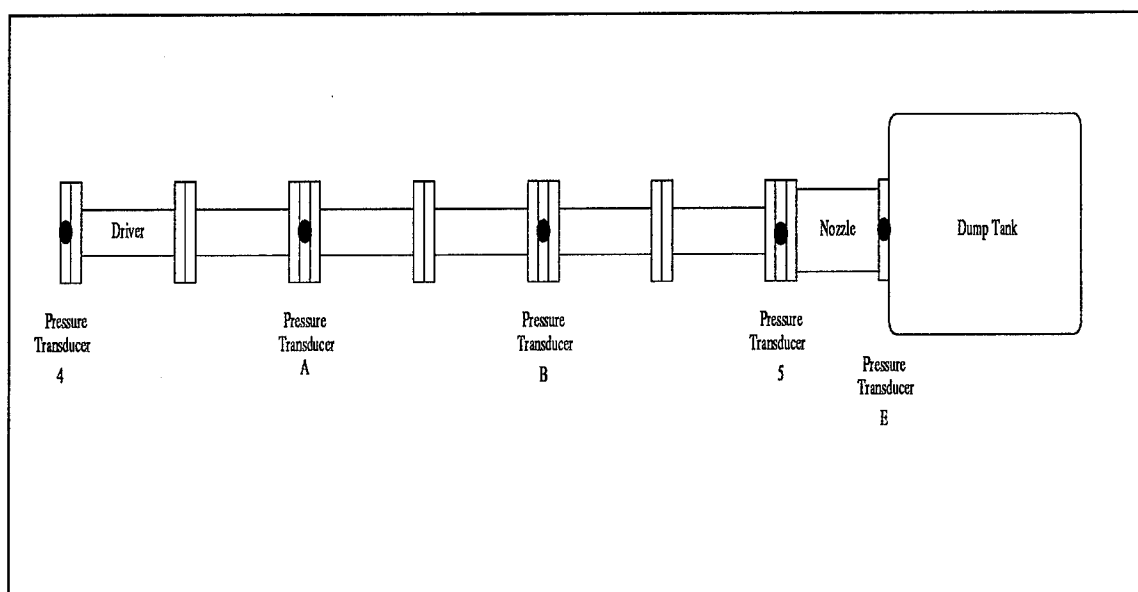


Figure 3. Pressure Transducer Locations

Figure 4 shows the incident shock passage and pressure jump to  $P_2$  followed almost immediately by a second pressure rise to  $P_5$  as the majority of the shock reflects from the entrance of the nozzle. Part of the shock wave passes through the nozzle, accelerating the air in the nozzle and helping to start the nozzle flow (Fig 5). Interested readers might refer to Zucrow (1976) or Sutton (1986) for specifics on nozzle flow. The steady flow condition exists until the pressure at the nozzle entrance ( $P_5$ ) drops below approximately 160 psi (1.10MPa) and the standing shock moves upstream to the pressure transducer location (at time 19.8 milliseconds on Fig 5). Figure 6 shows the pressure variation at the nozzle exit for a case where the pressure ratio  $P_5/P_1$  was not large enough to ‘start’ the nozzle.

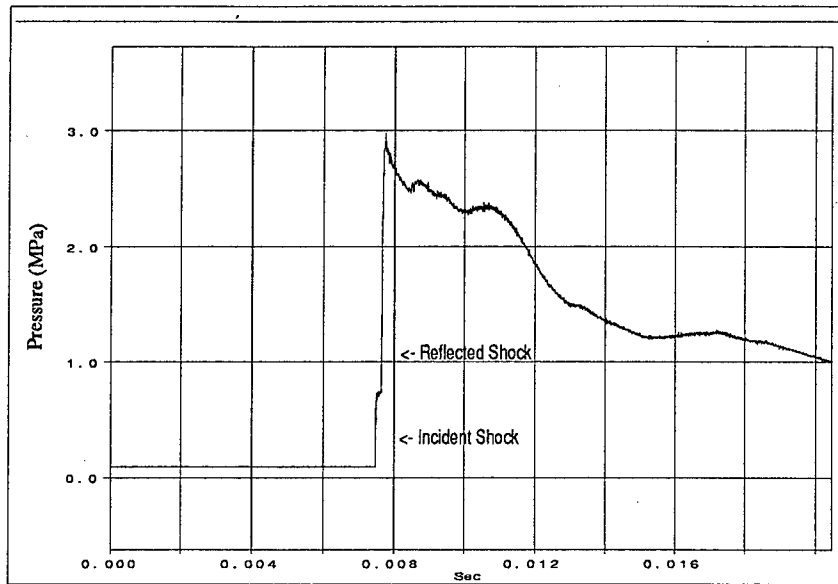


Figure 4. Pressure History at the Nozzle Entrance (Pressure Transducer 5)

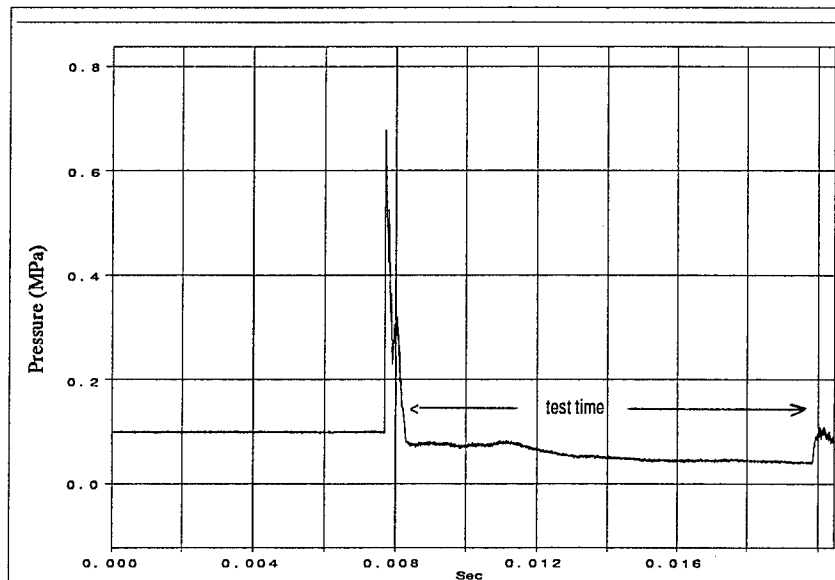


Figure 5. Pressure History at the Nozzle Exit (Pressure Transducer E)

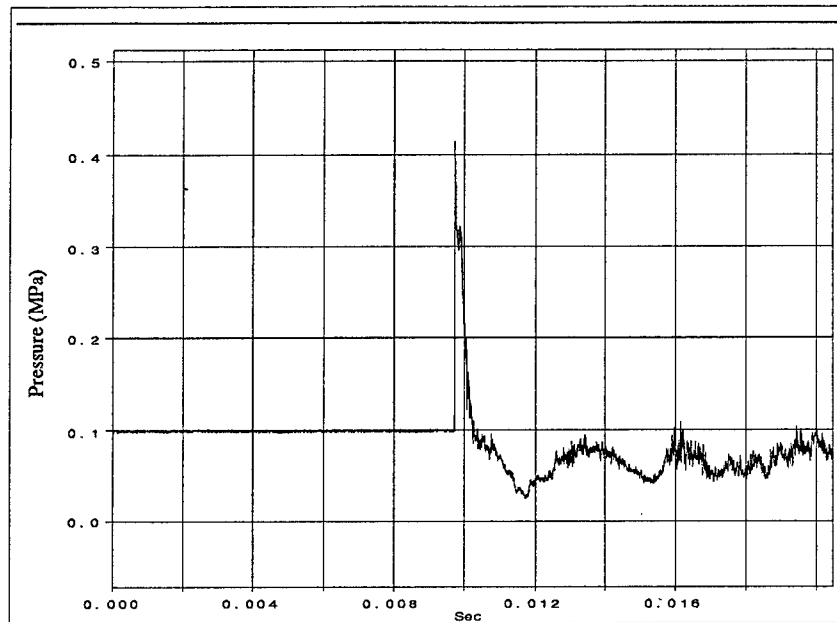


Figure 6. Pressure History at the Nozzle Exit for an Unstarted Nozzle

### *Comparison with Theory*

For this study, the driven pressure ( $P_1$ ) was 14.4 psi (0.10 MPa) for all data runs. The driver pressures varied from 400 psi to 1541 psi (2.76 MPa to 10.62 MPa). The majority of the shock waves were created using the two diaphragm technique although a few runs were accomplished using single diaphragms. No difference was noted in the data attributable to the use of one or two diaphragms. Similarly, most runs included the Mach 3 nozzle while a small number included a plate to serve as an endwall for the shock to reflect. The pressures behind the reflected shock waves were closer to theory for the attached endwall case as expected. The ideal curves represent a partial pressure of 14.4 psi of air in the shock tube driver section. The gas constant and ratio of specific heats of the driver gas were calculated for each test's

driver section gas makeup. They were not assumed to be equal to the values for pure helium, although they were assumed constant for the duration of each data run.

The shock strengths created were substantially less than predicted by the ideal shock tube equations. Figure 7 shows a comparison of the measured Mach number versus the diaphragm pressure ratio. The deviation from ideal is caused by losses incurred in the diaphragm rupturing process. The symbol 'o' represents the case in which the nozzle was attached to the shock tube. The symbol '+' represents the case in which the end of the shock tube was blocked by a flat plate serving as an endwall. It is important to keep these two cases in mind in later figures that involve the pressure behind the reflected shock wave. Since the nozzle does not completely reflect the shock, the data will show a larger discrepancy with the ideal case.

Figure 8 shows the pressure ratio across the incident shock versus the diaphragm pressure ratio. Both the Mach number and the shock strength could be used to measure the effectiveness of the shock tube in forming the shock wave, with the ideal shock relations providing a theoretical upper limit. Just as in Fig 7, there is a large data scatter due to inconsistencies in the diaphragm ruptures. Since some of the diaphragms opened more fully than others, they created shock waves closer to the predicted values.

Figure 9 shows measured Mach numbers and shock strengths versus normal shock theory (Eq 1) indicating the relative accuracy of the measured pressures and Mach numbers. The measured values of  $P_2$  followed closely to what normal shock relations predicted for the measured Mach number but were, on average, 30% below predictions based on ideal shock

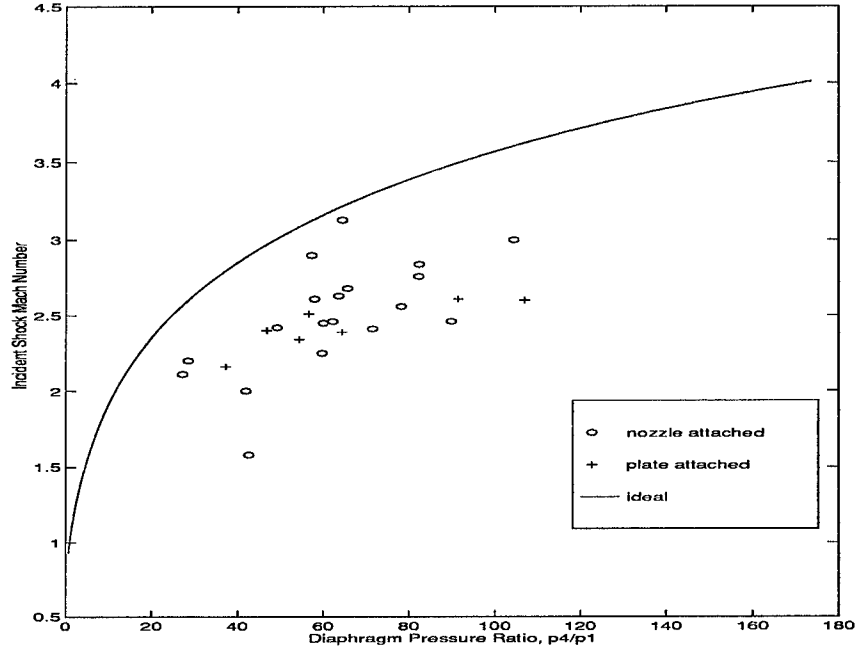


Figure 7. Incident Shock Wave Mach Number Versus Diaphragm Pressure Ratio Compared to Ideal Shock Tube Relations

tube relations for  $P_4/P_1$ . This was a consequence of the shock wave being slower and weaker than predicted by the ideal shock tube relations.

Figure 10 shows a comparison of the measured  $P_5/P_1$  pressure ratios with ideal predictions based upon the diaphragm pressure ratio. This data shows an average 65% lower pressure ratios behind the reflected shock wave than the ideal case. The two major contributors of the lower pressures was the initial loss from the diaphragm rupture and the less than perfect reflection of the shock wave on the nozzle. With the nozzle attached, a portion of the shock wave flowed through the throat of the nozzle rather than being reflected. This caused the reflected shock wave to be weaker. The shock wave flowing through the nozzle is depicted in Fig 5 as a sharp spike in the pressure just prior to the test time. Plotting  $P_5/P_1$  versus the

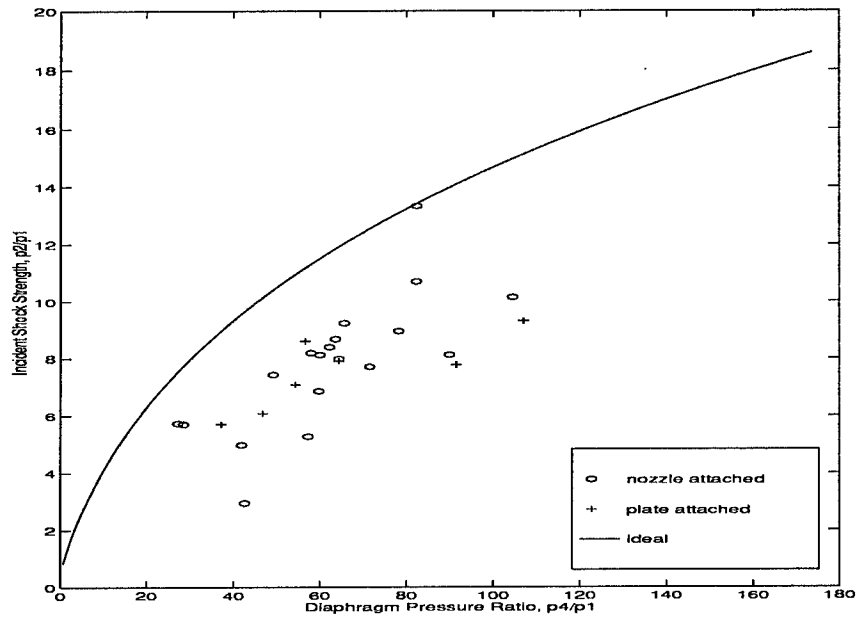


Figure 8. Incident Shock Strength Versus Diaphragm Pressure Ratio Compared to the Ideal Shock Tube Relations

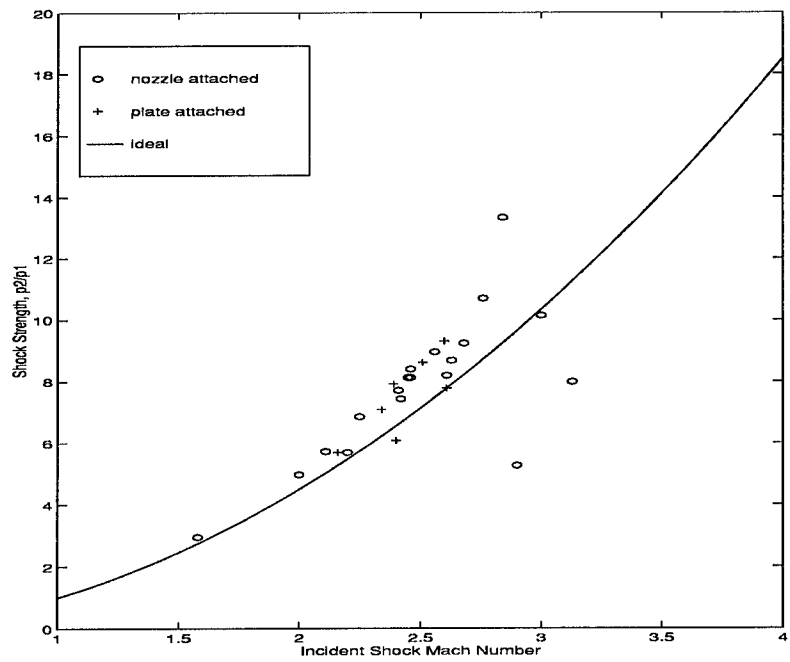


Figure 9. Incident Shock Strength Versus Mach Number



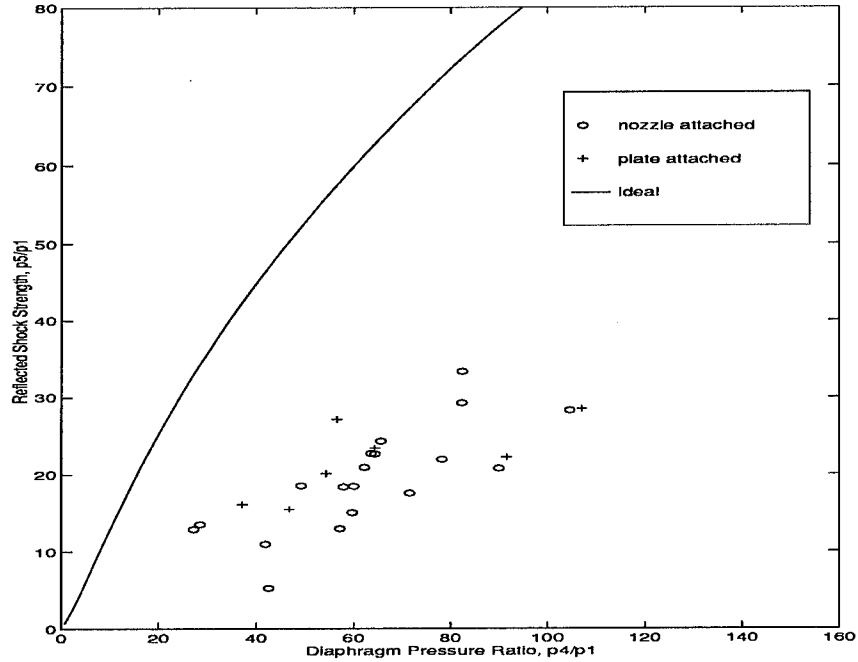


Figure 10. Reflected Shock Strength Versus Diaphragm Pressure Ratio Compared to the Ideal Shock Tube Relations

measured incident Mach numbers (Fig 11) eliminates the pressure losses associated with the formation of the shock wave discussed earlier.

Data runs were made both with and without a nozzle to determine if the nozzle created significant reductions in the reflected shock strengths. Figure 11 shows the ideal curve for  $P_5/P_1$  calculated from the measured incident shock Mach numbers and clearly indicates that the nozzle did have an effect on the shock wave reflection. The data tends to form two lines, both following the predicted trend. The line of points representing the case of the attached nozzle (o) is farther from the ideal curve. This figure shows an average pressure loss of only 10% compared with ideal for the attached plate and 31% loss for the attached nozzle.

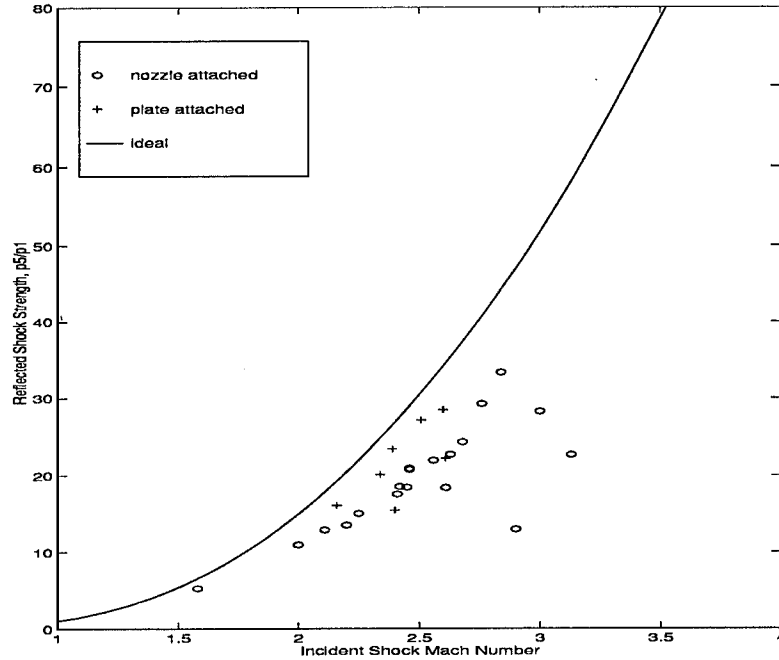


Figure 11. Incident Shock Mach Number Versus Reflected Shock Strength Compared to the Ideal Shock Tube Relations

A number of studies have been conducted using the 2-inch shock tube but only Baer (1982) included a comparison of his data to theory. The current study's data as depicted in Fig 7 compares favorably to Baer's data (Fig 12), suggesting that the shock tube performed similarly for both studies. Similar losses were undoubtedly incurred in the other studies, but this problem was not discussed. It should be noted that Baer's curve representing the ideal relations differs from this work's due to his use of argon as his driven gas. Figure 13 shows Baer's data for  $P_5/P_1$  versus Mach number (compare this to Fig 11 noting that the axes are reversed). Approximately one third of the data points show  $P_5$  exceeding the theoretical limit. Because of this and the large spread in his data, it would be difficult to draw any conclusions based upon Baer's data for pressures behind the reflected shock wave.

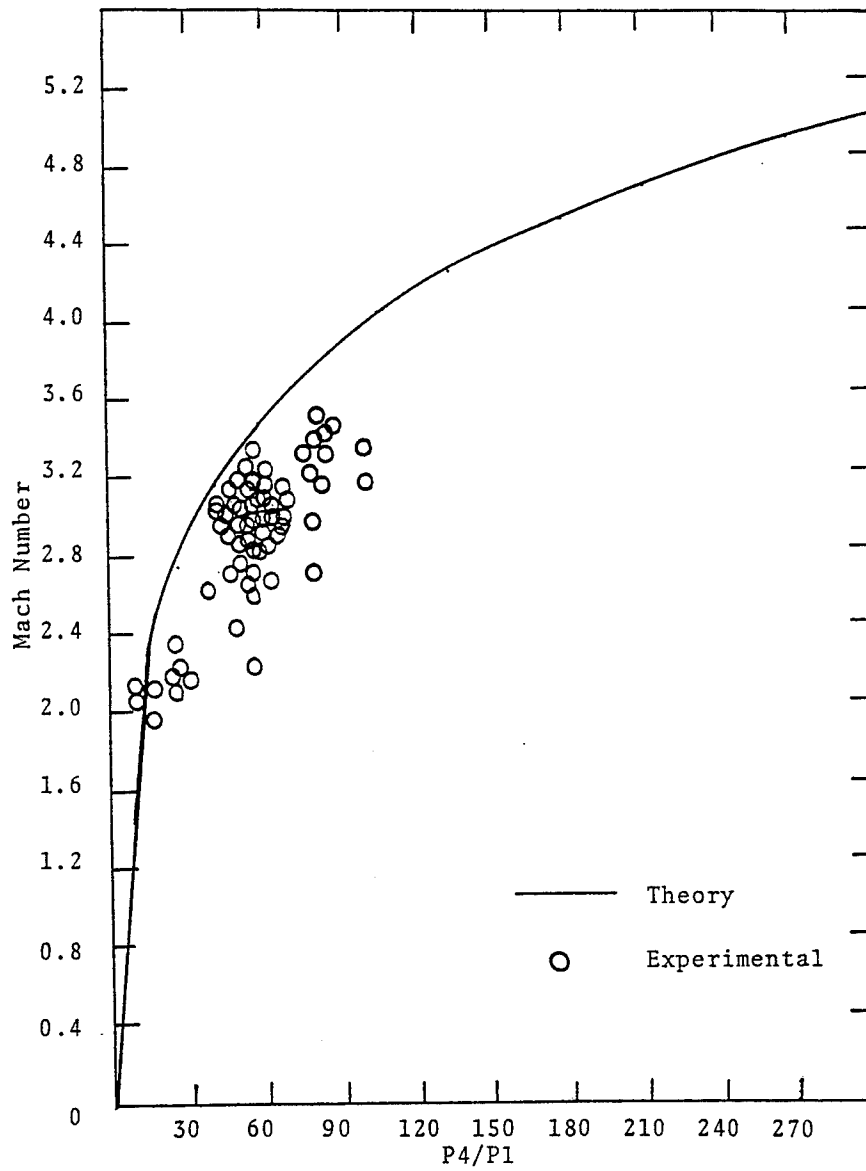


Figure 12. Baer's Figure 11, P4/P1 vs Mach Number

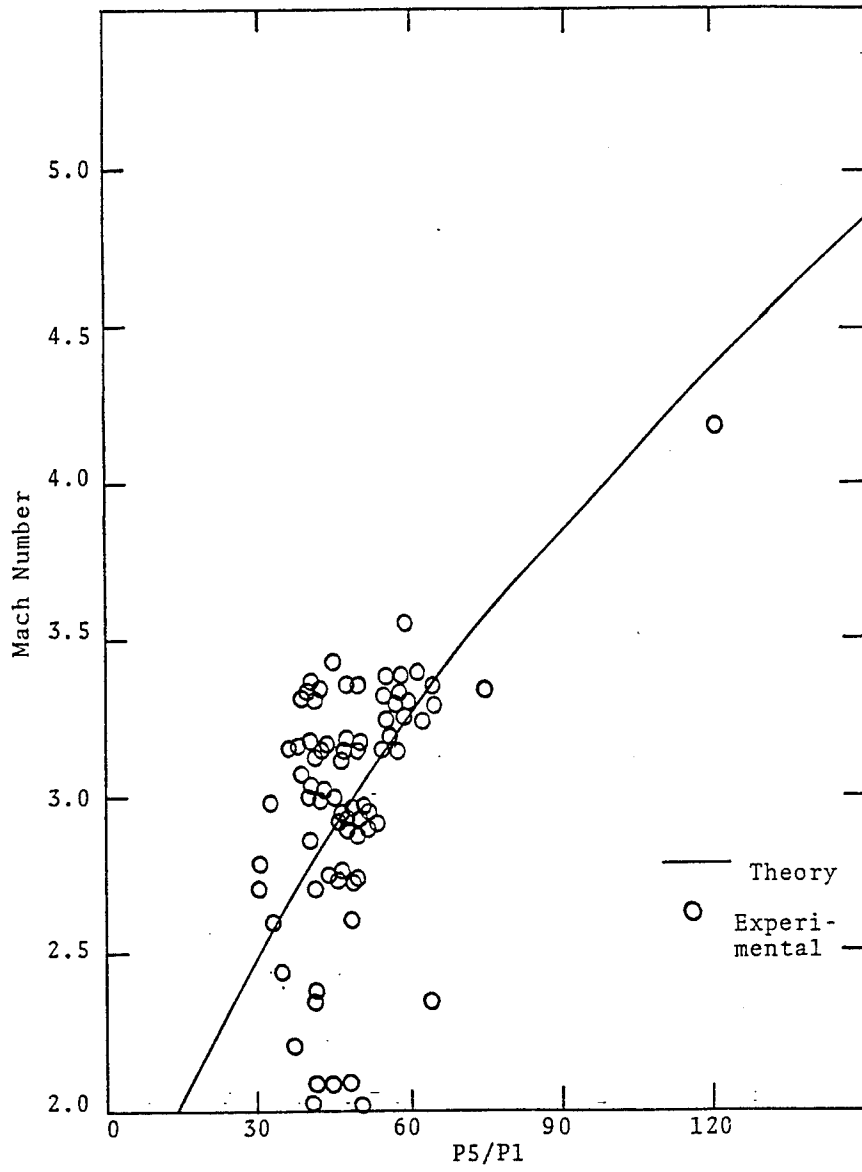


Figure 13. Baer's Figure 12, P5/P1 vs Mach Number

Uda (1968) used a 3-inch shock tube and showed measured Mach numbers of the incident shock wave 15-20% below predicted values (Fig 14). Using the measured Mach numbers eliminates carrying this discrepancy into the predictions for the pressure behind the reflected shock. Uda's figure for  $P_5/P_1$  vs. shock Mach number (Fig 15) closely follows the ideal curve. This was good justification for assuming that the ideal shock tube relations accurately described his flow and that the temperatures behind the reflected shock waves also followed theory.

#### *Test Times*

Test times were determined by the period of steady flow measured by the pressure transducer located in the nozzle exit plane. Although the critical pressure ratio, the pressure ratio required to fully expand the flow to Mach 3, was never achieved, a sufficient pressure ratio  $P_5/P_1$  was obtained to start the nozzle. For this case the driven gas reached Mach 3 in an overexpanded flow condition. As the pressure at the nozzle entrance dropped, a standing shock formed in the diverging nozzle section to increase the overexpanded flow pressure back to ambient. This standing shock wave moved slowly upstream with decreasing  $P_5$ . The test time was then the time between nozzle start-up and standing shock encroachment.

With the Mach 3 nozzle attached, the test times measured ranged from 4 to 12 milliseconds. The pressure threshold required to maintain steady flow without interruption by a standing shock wave in the nozzle was experimentally determined to be 150–160 psi (1.03–1.10 MPa). The test time duration depended upon the time that  $P_5$  stayed above the threshold.

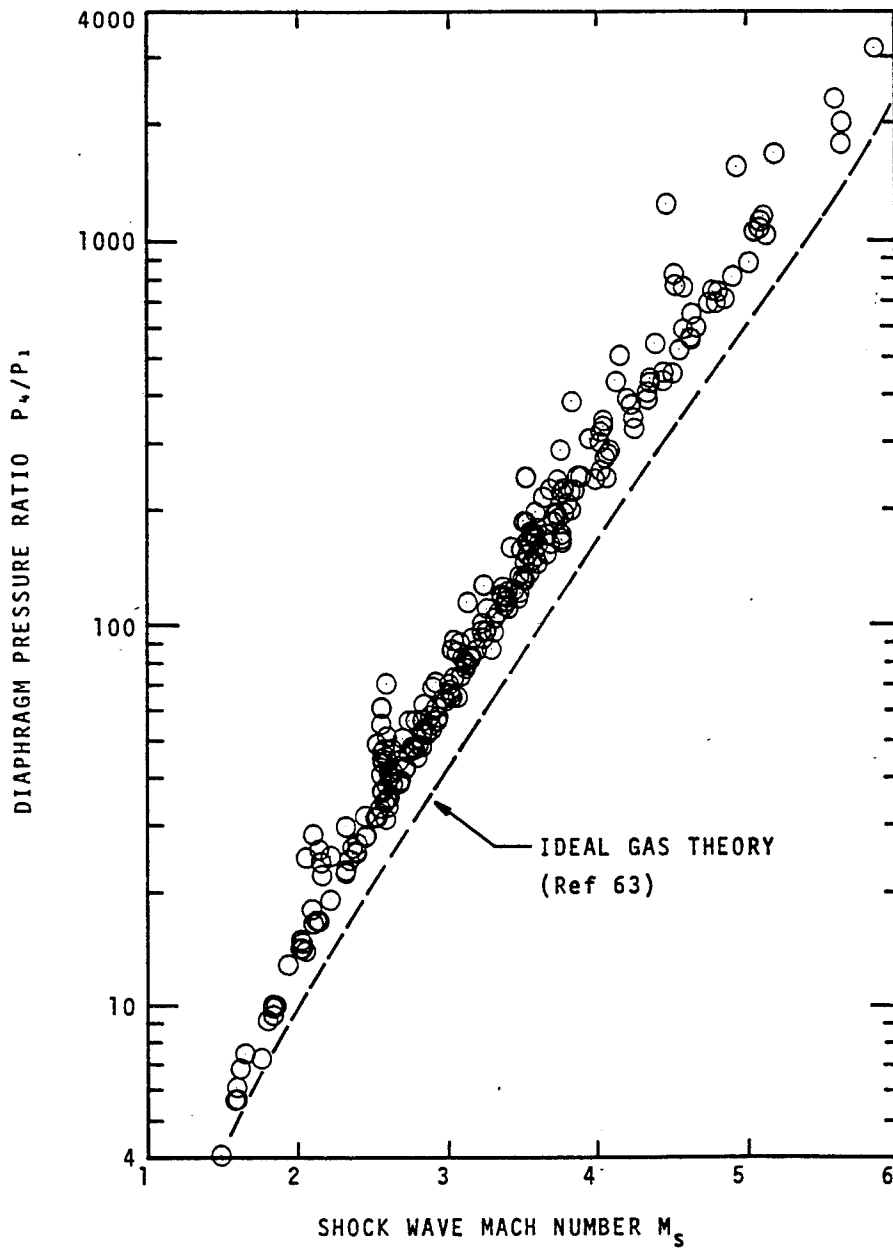


Figure 14. Uda's Figure 22, Diaphragm Pressure Ratio Experimental Data Points Compared to Ideal Gas Theory Curve for the He/Air System

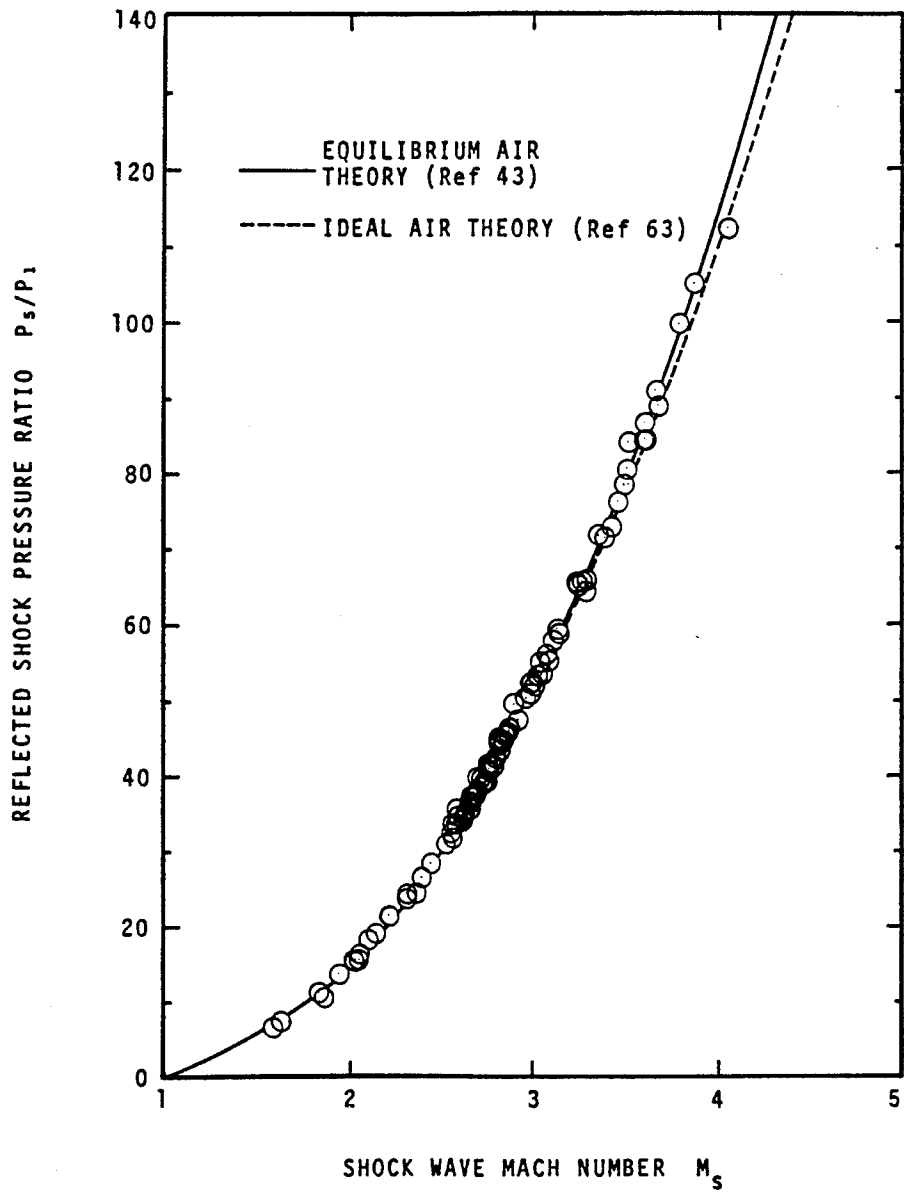


Figure 15. Uda's Figure 23, Reflected Shock Pressure Ratio Experimental Data Points Compared to Equilibrium and Ideal Air Theory Curves

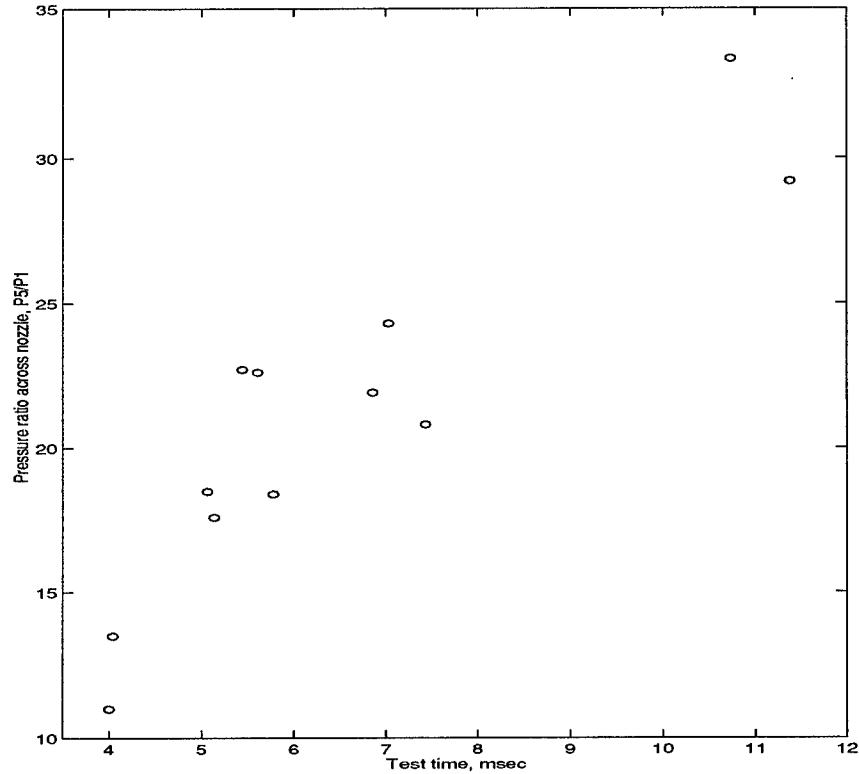


Figure 16. Measured Test Times as a Function of the Pressure Ratio Across the Nozzle

The time  $P_5$  remained above the threshold was proportional to the initial  $P_5$  attained. Figure 16 shows the measured test times as a function of the initial pressure ratio across the nozzle  $P_5/P_1$ . Flow duration could be affected by the contact surface (and therefore the driver gas) flowing through the nozzle and entering the test section. Since the driver gas is at a lower temperature and may have a different specific heat ratio if the driver and driven gases differ (as in the case of the present study), the data collected after this point may no longer be useable. This was determined not to be the case for the present study but could be a factor if higher pressures behind the reflected shock are obtained.



To verify that the test time was not shortened by the arrival of the contact surface in the test section, the mass flow rate of the nozzle was calculated and compared to the amount of air in the nozzle prior to diaphragm rupture. Once an amount of mass equal to the mass of air initially in the shock tube has flowed through the nozzle, driver gas must necessarily be entering the test section.

Assuming an isentropic nozzle, the mass flow rate ( $\dot{m}$ ) is determined from (Sutton, 1986)

$$\dot{m} = A_t P_5 \frac{\gamma \sqrt{\left(\frac{2}{\gamma+1}\right)^{\frac{\gamma+1}{\gamma-1}}}}{\sqrt{\gamma R T_5}} \quad (8)$$

where  $A_t$  is the throat area and  $P_5$  and  $T_5$  are taken to be the 'chamber' pressure and temperature. For air as the test gas and a throat area of  $0.000343 \text{ m}^2$ , this can be reduced to

$$\dot{m} = 1.3854 \times 10^{-5} \frac{P_5}{\sqrt{T_5}} \quad (9)$$

where pressure is in pascals, temperature in degrees kelvin, and  $\dot{m}$  in kg/sec.

The chamber conditions are taken to be the same as the conditions initially behind the reflected shock,  $P_5$  and  $T_5$ . Since the pressure and presumably the temperature are not constant during the test interval,  $\dot{m}$  is a time varying unknown and each test run will be different. Noting that  $\dot{m}$  varies proportionally with pressure, the time to deplete the *air* in the tube decreases with increasing pressure.

To confirm that none of the measured test times included flow of driver gas through the nozzle, a few of the longest test times were verified to be shorter than the depletion time and the shorter test times were then considered to be indirectly verified. As an example of this verification procedure, the calculations for one of the data runs are repeated below.

For a test run producing a test time of 11.38 msec, the driver pressure was 1185 psia (8.17 MPa) with driven pressure at one atmosphere. From Fig 17,  $P_2$  was determined to be 154 psia (1.06 MPa) and from Fig 4,  $P_5$  peaks at 420 psia (2.90 MPa).  $P_5$  was 30% below its predicted value based upon the measured shock wave Mach number. The chamber pressure quickly dropped below 400 psia (2.76 MPa) but in the interest of calculating a conservative estimate, it was assumed that the pressure remained constant at 400 psia. In actuality, the pressure was lower than 400 psia the majority of the time, which lowers the mass flow rate and increases the time for air depletion.

Assuming a temperature behind the reflected shock 30% lower than predicted, similar to the pressure,  $T_5$  was estimated to be 70% of the temperature predicted by the ideal shock relations. From Eq 7 with a Mach number of 2.76 and an initial temperature  $T_1$  of 298 K,  $T_5$  was predicted to be 1232 K and with the 70% estimation,  $T_5$  was taken to be 862 K. Equation 9 then leads to an air mass flow rate of 1.366 kg/s.

From the thermal equation of state, the density of air at 14.4 psi (.10 MPa) was found to be 1.16 kg/m<sup>3</sup>. For a driven section volume of  $1.556 \times 10^{-2}$  m<sup>3</sup>, the initial mass of air in the shock tube was  $1.81 \times 10^{-2}$  kg. Dividing the mass by the mass flow rate, an estimate of the air depletion time was found to be 13.2 milliseconds.

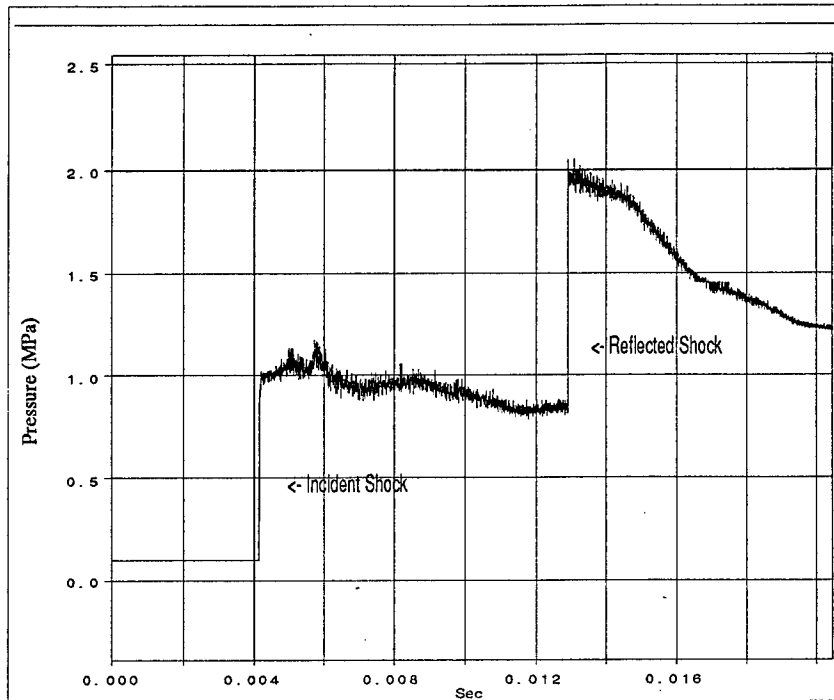


Figure 17. Pressure History at the Location of Pressure Transducer B Upstream of the Nozzle

The test time for this run safely ended prior to any corruption introduced by interaction with the driver gas. However, if the pressure at the nozzle was increased to maintain a steady flow duration greater than 12 msec, the mass flow rate of the air through the nozzle would also increase and the air would be depleted in less time. With this in mind, it appears that the maximum obtainable test time for initial driven gas pressure at one atmosphere is 12 to 14 msec.

### *Nozzle Mach Numbers*

The Mach number in the test section was calculated based upon the assumption of isentropic expansion of the air through the nozzle. For one-dimensional isentropic flow of a perfect gas (Zucrow, 1976:173)

$$\frac{P_5}{p_e} = \left(1 + \frac{\gamma - 1}{2} M_e^2\right)^{\frac{\gamma}{\gamma - 1}} \quad (10)$$

where  $P_5$  is the stagnation pressure,  $p_e$  is the static pressure at the nozzle exit, and  $M_e$  is the Mach number at the nozzle exit. Both  $p_e$  and  $P_5$  were measured during the test time and Mach numbers were then calculated. Mach numbers varied during the test time from beginning values of 2.92 - 2.96 and trailing off to values of 2.74 to 2.78 at the end of the test time. Higher pressures behind the reflected shock wave may reduce this variation of Mach number by keeping the nozzle underexpanded for the duration of the test time. The pressure in the test section also decreased during the test time, on average 6 psia (41.4 kPa), as was shown in Fig 5.

## *V. Conclusions and Recommendations*

### *Conclusions*

The flow in the AFIT 2-inch shock tube is poorly represented by the ideal relations for shock tubes based only upon the initial driver-to-driven pressure ratio. The pressure rise behind the incident shock wave was, on average, 30% less than predicted by theory. Pressures behind the reflected shock were 65% below ideal based upon  $P_4/P_1$ . When based upon the measured Mach number of the incident shock wave to eliminate losses due to the diaphragm rupture process, the pressure loss behind the reflected shock was reduced to 31% for the case of the attached Mach 3 nozzle. This does not prevent the shock tube from providing useable test times, but makes it less efficient and uses more helium.

During this study, the AFIT 2-inch shock tube with an attached Mach 3 nozzle provided 4 to 12 milliseconds of steady flow in the test section for an initial driven gas at atmospheric pressure and initial driver pressures ranging from 400 to 1541 psi (2.76 to 10.62 MPa). 12 to 14 msec is believed to be the maximum obtainable test time for initial driven gas pressure at atmosphere. The higher pressures required for a longer flow duration increase the mass flow rate of the air through the nozzle and decrease the amount of time necessary for all the air initially in the shock tube to evacuate.

### *Recommendations*

A vacuum system could be used to get higher driver-to-driven ( $P_4/P_1$ ) pressure ratios. This would expand the range of  $P_4/P_1$  and  $P_5/P_1$  pressure ratios obtainable. It would also allow  $P_5/P_1$  ratios to be reached with a lower driver pressure, thereby using less driver gas. The drawback to this is that there is less driven gas in the shock tube and test durations will be shortened. If the driver gas is the same as driven for studies where the temperature difference behind the contact surface will not adversely affect the data, the test times would not be cut short by the arrival of the contact surface and the duration of steady flow might be increased above 14 msec.

A new pressure regulator for the shock tube driver supply system should be obtained in order to supply a driver pressure greater than 1500 psi (10.34 MPa) and exceed the critical pressure ratio of the nozzle. This would also expand the range of obtainable driver-to-driven pressure ratios.

Higher quality diaphragms must be obtained in order to produce more consistent and predictable ruptures. This would prevent premature ruptures, saving driver gas, time and diaphragms. In addition, it would permit the use of driver pressures closer to the breaking strength of the diaphragm which would result in better ruptures. The diaphragms used for this study had breaking strengths that varied as much as a third of the maximum.

## *Appendix A. Data*

The following two tables list the data used in the calculations and figures throughout this study. Data from runs where the diaphragms ruptured prematurely or the data was otherwise flawed, is not included below nor in any of the preceding figures

Table 1. Data for the Case of the Nozzle Attached

$P_4$ psi/MPa	$P_1$ psi/MPa	$P_2$ psi/MPa	$P_5$ psi/MPa	Mach number
410 / 2.83	14.4 / 0.10	82.0 / 0.57	195 / 1.34	2.23
824 / 5.68	14.4 / 0.10	75.9 / 0.52	187 / 1.29	2.89
1505 / 10.38	14.4 / 0.10	146 / 1.01	407 / 2.81	2.97
604 / 4.16	14.4 / 0.10	71.6 / 0.49	158 / 1.09	2.00
928 / 6.40	14.4 / 0.10	115 / 0.79	326 / 2.25	3.13
945 / 6.52	14.4 / 0.10	133 / 0.92	350 / 2.41	2.68
834 / 5.75	14.4 / 0.10	118 / 0.81	265 / 1.83	2.61
916 / 6.32	14.4 / 0.10	125 / 0.86	327 / 2.25	2.63
860 / 5.93	14.4 / 0.10	98.7 / 0.68	217 / 1.50	2.25
864 / 5.96	14.4 / 0.10	117 / 0.81	266 / 1.83	2.45
896 / 6.18	14.4 / 0.10	121 / 0.83	301 / 2.08	2.46
1185 / 8.17	14.4 / 0.10	154 / 1.06	421 / 2.90	2.76
1294 / 8.92	14.4 / 0.10	117 / 0.81	299 / 2.06	2.46
1126 / 7.76	14.4 / 0.10	129 / 0.89	316 / 2.18	2.56
1187 / 8.18	14.4 / 0.10	192 / 1.32	480 / 3.31	2.84
392 / 2.70	14.4 / 0.10	82.5 / 0.57	186 / 1.28	2.11
709 / 4.89	14.4 / 0.10	107 / 0.74	267 / 1.84	2.42
613 / 4.23	14.4 / 0.10	44.9 / 0.31	76 / 0.52	1.58
1030 / 7.10	14.4 / 0.10	111 / 0.77	253 / 1.74	2.41

Table 2. Data for the Case of the Plate/Endwall Attached

$P_4$ psi/MPa	$P_1$ psi/MPa	$P_2$ psi/MPa	$P_5$ psi/MPa	Mach number
674 / 4.65	14.4 / 0.10	87.5 / 0.60	223 / 1.54	2.40
815 / 5.62	14.4 / 0.10	114 / 0.79	391 / 2.70	2.51
784 / 5.41	14.4 / 0.10	134 / 0.92	290 / 2.00	2.34
927 / 6.39	14.4 / 0.10	112 / 0.77	337 / 2.32	2.39
1541 / 10.62	14.4 / 0.10	82 / 0.57	410 / 2.83	2.60
1302 / 8.98	14.4 / 0.10	124 / 0.85	320 / 2.21	2.61
536 / 3.70	14.4 / 0.10	102 / 0.70	232 / 1.60	2.16



## Bibliography

1. *DADiSP Worksheet, Data Analysis and Display Software*. User Manual. Cambridge: DSP Development Corporation, 1992.
2. Baer, James J. *Spectrographic Analysis of Iodine Emission*. MS thesis, School of Engineering, Air Force Institute of Technology, 1982.
3. Farnell, Lawrence C. *Iodine Dissociation in a Shock Tube*. MS thesis, School of Engineering, Air Force Institute of Technology, 1980.
4. Gaydon, A.G. and I.R. Hurlle. *The Shock Tube in High Temperature Chemical Physics*. New York: Reinhold Publishing Corp, 1963.
5. Glass, I.I. and J. Hall. *Shock Tubes, Part I and II*. Toronto: University of Toronto, Institute of Aerophysics, 1958.
6. Jones, James T. *Boron Ignition Limit Curve as Determined by a Shock Tube Study*. MS thesis, School of Engineering, Air Force Institute of Technology, 1969.
7. Sutton, George P. *Rocket Propulsion Elements*. New York: John Wiley & Sons, 1986.
8. Uda, Robert T. *A Shock Tube Study of the Ignition Limit of Boron Particles*. MS thesis, School of Engineering, Air Force Institute of Technology, 1968.
9. Zucrow, Maurice J. and Joe D. Hoffman. *Gas Dynamics, Vol I.*. New York: John Wiley & Sons, 1976.

## *Vita*

Captain Kevin M. Vlcek was born on January 4, 1966 on Bitburg AB, West Germany. He graduated from high school in Springfield, Ohio in 1984 and attended the University of Michigan from which he received the degree of Bachelor of Science in Aerospace Engineering in April 1988. Upon graduation, he received a commission in the USAF through the Reserve Officers Training Corps (ROTC).

In March of 1989, Captain Vlcek graduated from Undergraduate Space Training, Lowry AFB, Colorado. After four years of satellite operations for the Defense Support Program (DSP) and Defense Meteorological Satellite Program (DMSP) at the 1st Space Operations Squadron, 50th Space Wing, AFSPACECOM, Falcon AFB, Colorado, Captain Vlcek entered the Graduate School of Engineering, Air Force Institute of Technology, Wright-Patterson AFB, Ohio.

Permanent address: 5659 S. Tecumseh Rd.  
Springfield, Ohio 45502

December 1994

Master's Thesis

AN INVESTIGATION OF THE AFIT 2-INCH SHOCK TUBE AS A FLOW  
SOURCE FOR SUPERSONIC TESTING

Kevin M. Vlcek  
Capt, USAF

Air Force Institute of Technology  
Wright-Patterson AFB OH 45433-6583

AFIT/GA/ENY/94D-1

L. Kevin Sponsor  
PL/VTS  
Kirtland AFB, NM 87117-5776

WILLIAM P. JOHNSON  
WL / FIBEE  
WEIGHT-PATERSON AFB, OH 45433

Approved for public release; distribution unlimited

An investigation of the AFIT high pressure shock tube was conducted to determine how closely it followed ideal shock tube theory and to determine the available test times for an attached Mach 3 nozzle. The driver section was five feet (1.52 m) long and the driven section was 25 feet (7.62 m) long. The driver gas used for this study was helium while the driven gas was atmospheric air. The pressure rise measured behind the incident shock wave was, on average, 30% lower than predicted by the ideal shock tube relations. Behind the reflected shock, the pressure rise was 65% lower than predictions based on initial driver gas pressure. Due to supply pressure limits and lower than predicted pressures behind the shock waves, fully expanded flow in the Mach 3 nozzle was not attained. However, steady overexpanded flows of Mach 2.74–2.96 were observed for periods of 4–12 milliseconds.

Shock Tubes, Shock Tunnels, Nozzles, Shock Waves

164

UNCLASSIFIED

UNCLASSIFIED

UNCLASSIFIED

UL

# REPORT DOCUMENTATION PAGE

Form Approved  
OMB No. 0704-0188

Public reporting burden for this collection of information is estimated to average 1 hour per response, including the time for reviewing instructions, searching existing data sources, gathering and maintaining the data needed, and completing and reviewing the collection of information. Send comments regarding this burden estimate or any other aspect of this collection of information, including suggestions for reducing this burden, to Washington Headquarters Services, Directorate for Information Operations and Reports, 1215 Jefferson Davis Highway, Suite 1204, Arlington, VA 22202-4302, and to the Office of Management and Budget, Paperwork Reduction Project (0704-0188), Washington, DC 20503.

<b>1. AGENCY USE ONLY (Leave blank)</b>		<b>2. REPORT DATE</b> December 1994	<b>3. REPORT TYPE AND DATES COVERED</b> Master's Thesis	
<b>4. TITLE AND SUBTITLE</b> AN INVESTIGATION OF THE AFIT 2-INCH SHOCK TUBE AS A FLOW SOURCE FOR SUPERSONIC TESTING			<b>5. FUNDING NUMBERS</b>	
<b>6. AUTHOR(S)</b> Kevin M. Vlcek Capt, USAF				
<b>7. PERFORMING ORGANIZATION NAME(S) AND ADDRESS(ES)</b> Air Force Institute of Technology Wright-Patterson AFB OH 45433-6583			<b>8. PERFORMING ORGANIZATION REPORT NUMBER</b> AFIT/GA/ENY/94D-1	
<b>9. SPONSORING / MONITORING AGENCY NAME(S) AND ADDRESS(ES)</b> William P. Johnson WL/FIBEB Wright-Patterson AFB, OH 45433			<b>10. SPONSORING / MONITORING AGENCY REPORT NUMBER</b>	
<b>11. SUPPLEMENTARY NOTES</b>				
<b>12a. DISTRIBUTION / AVAILABILITY STATEMENT</b> Approved for public release; distribution unlimited			<b>12b. DISTRIBUTION CODE</b>	
<b>13. ABSTRACT (Maximum 200 words)</b> An investigation of the AFIT high pressure shock tube was conducted to determine how closely it followed ideal shock tube theory and to determine the available test times for an attached Mach 3 nozzle. The driver section was five feet (1.52 m) long and the driven section was 25 feet (7.62 m) long. The driver gas used for this study was helium while the driven gas was atmospheric air. The pressure rise measured behind the incident shock wave was, on average, 30% lower than predicted by the ideal shock tube relations. Behind the reflected shock, the pressure rise was 65% lower than predictions based on initial driver gas pressure. Due to supply pressure limits and lower than predicted pressures behind the shock waves, fully expanded flow in the Mach 3 nozzle was not attained. However, steady overexpanded flows of Mach 2.74-2.96 were observed for periods of 4-12 milliseconds.				
<b>14. SUBJECT TERMS</b> Shock Tubes, Shock Tunnels, Nozzles, Shock Waves			<b>15. NUMBER OF PAGES</b> 164	
			<b>16. PRICE CODE</b>	
<b>17. SECURITY CLASSIFICATION OF REPORT</b> UNCLASSIFIED	<b>18. SECURITY CLASSIFICATION OF THIS PAGE</b> UNCLASSIFIED	<b>19. SECURITY CLASSIFICATION OF ABSTRACT</b> UNCLASSIFIED	<b>20. LIMITATION OF ABSTRACT</b> UL	